FUNCTIONAL WATER CHANNELS WITHIN THE TSH RECEPTOR – a new paradigm for TSH action with disease implications

Authors: Rauf Latif [1,2], Terry F. Davies[1,2] and Mihaly Mezei[1,3*]

[1]Thyroid Research Unit, Department of Medicine, Icahn School of Medicine at Mount Sinai; New York, NY
[2]James J. Peters VA Medical Center; New York, NY.
[3]Department of Pharmacological Sciences, Icahn School of Medicine at Mount Sinai; New York, NY

*__Corresponding author__. Email: Mihaly.Mezei@mssm.edu

ORCID numbers: 0000-0003-0294-4307 (M. Mezei); 0000-0002-4226-3728 (R. Latif), and 0000-0003-3909-2750 (T.F. Davies).

Competing interests: TFD is a member of the Board of Kronus Inc, Starr, Idaho; MM & RL have no competing interest.

Funding: Veterans Administration (VA) Merit Award BX000800 (TFD)
Anonymous philanthropic donations (TFD).

Keywords: TSHR, GPCR, DPPC, molecular dynamics, water channel, calcein**.**

Abstract: The TSH receptor (TSHR) transmembrane domain (TMD) lives in the plasma membrane consisting of lipids and water molecules. To understand the role of TSHR-associated water molecules we used molecular dynamic simulations of the TMD and identified a network of putative receptor associated transmembrane water channels. This result was confirmed with extended simulations of the full length TSHR with and without TSH ligand binding. While the transport time observed in the simulations via the TSHR protein was slower than via the lipid bilayer itself we found that significantly more waters traversed via the TSHR than via the lipid bilayer which more than doubled with the binding of TSH. Using rat thyroid cells (FRTL-5) and a calcein fluorescence technique we measured cell volumes after blockade of aquaporins 1 and 4, the major thyroid cell water transporters. TSH showed a dose-dependent ability to influence water transport and similar effects were observed with stimulating TSHR autoantibodies. Small molecule TSHR agonists, which are allosteric activators of the TMD, also enhanced water transport illustrating the role of the TMD in this phenomenon. Furthermore, the water channel pathway was also mapped across two activation motifs within the TSHR TMD suggesting how water movement may influence activation of the receptor. In pathophysiological conditions such as hypothyroidism and hyperthyroidism where TSH concentrations are highly variable this action of TSH may greatly influence water movement in thyroid cells and many other extrathyroidal sites where the TSHR is expressed thus affecting normal cellular function.

INTRODUCTION

The thyroid-stimulating hormone receptor (TSHR) is a membrane-bound glycoprotein sharing a common architecture with other members of the G-protein coupled receptor (GPCR) family with seven transmembrane helices making up the transmembrane domain (TMD). Similar to other GPCRs, the general activation process of the TSHR involves re-arrangement of these transmembrane helices and its association with other membrane protein partners and includes dimeric forms (1,2). Although it is known that a network of intramolecular and water-mediated interactions are important for stabilizing GPCR structures by linking the transmembrane helices (3-5) such associations of water channels within the TSHR nor other glycoprotein hormone receptors have not been examined.

Recently, we developed a computational model of the TSHR transmembrane domain (TMD) called TSHR-TMD-TRIO (6) which was based on molecular dynamics simulation. This dynamic model consisted of three representative structures extracted from a 600 ns molecular dynamics (MD) simulation of the TSHR TMD embedded in a dipalmitoyl-phosphatidyl-choline (DPPC) membrane and solvated with water, as well as counterions, to ensure neutrality and physiological ionic strength. The simulation preserved the seven-helix transmembrane bundle. The backbone of the third model of TRIO (that led us to the question whether the TSHR TMD can serve as a water channel) was superimposed on the corresponding atoms of the cryoEM models that were available (7) resulting in RMSDs of 6.3, 5.9 and 5.7 Å for PDB ids 7xw5, 7xw6, 7xw7, respectively. The C-terminal tail was not included but the loops connecting the helices were. In the present work we first examined this model for water that may enter the interior of the TMD. We obtained water positions in the TMD's interior based on the concept of generic water sites (8). Such sites are places whose vicinity most likely contains a water molecule. These calculations

revealed a contiguous chain of waters across the TMD. Examination of the same MD simulation that produced the TRIO model for the movements of waters during the simulation showed waters crossing the cell membrane through the TMD and also through the DPPC membrane bilayer. Biological support for these events was then obtained using an intracellular calcein fluorescence technique to detect changes in thyroid cell volume caused by water flux (see **Figure 1** and METHODS section below) which confirmed that in the presence of aquaporin blockade the TSH ligand was able to induce marked changes in cell volume, indicative of water transfer. Together these data indicate the presence of functional water channels within the TSHR-TMD and may reveal important new consequences of TSH action.

MATERIALS AND METHODS

The TSHR-TMD-TRIO model: The calculations started with our TMD model as described previously (9) which used the Uniprot server (10) to obtain an initial model of the seven transmembrane helices using the rhodopsin model (PDB:1F88) as the template. We generated the loops connecting the helices with a Monte Carlo procedure (11). Water molecules inside the TMD were obtained as generic sites (8) based on a grand-canonical ensemble Monte Carlo simulation (12). Such simulations vary the number of waters using periodic insertion and deletion attempts, and are accepted based on the Boltzmann factor including a target chemical potential that was obtained by tuning to experimental density in the bulk (13); generic sites represent density maxima of the water positions generated by the simulation. We then generated the membrane environment (vide infra), equilibrated the system and first performed a 600 ns molecular dynamics simulation. The TMD conformations generated by the MD run were clustered, using the backbone root mean square deviation (RMSD) method, as the distance measured using Simulaid (14). This indicated

the presence of clusters. Since the first cluster had few members it was discarded and additional equilibration and representatives were selected only from the three larger clusters - hence we gave it the name TSHR-TMD-TRIO (6).

The membrane model: As described in our earlier publication, the TSHR protein structure with internal waters was then submitted to the Charmm-Gui server (15). The server immersed the protein into a bilayer of 188 DPPC molecules and added a further water layer, resulting in a total of 15,277 waters, and also added counterions (40 K+ and 52 Cl- ions), both to ensure electroneutrality and an ionic strength of 0.15 to represent physiological conditions. The Charmm-36 force field (16) was used. This approach also provided the input for a six-step equilibration of the system that involved the progressive release of constraints on all non-water components in the system (17) to ensure that releasing local strains did not compromise the overall fold of the protein. The simulations were performed with the program NAMD (18).

Generic water sites: The calculation of the generic sites was an iterative process using a well-defined algorithm (8). Starting from the first conformation for each structure in the trajectory this algorithm assigned each water to a site or, if no suitable site was found, assigned it to a new putative site. The process was then repeated until the sites no longer changed and converged. The algorithm assigned to each site a fractional occupancy and RMSD (8). These calculations were performed by the program MMC (19).

Membrane transits: Using the program Simulaid (14) the trajectory was scanned for waters entering and exiting the membrane. Each time a water entered, its position and structure number was noted. Each time a water exited, the program recorded a successful transit if the exit occurred at the membrane side opposite the entry. The entry and exit points were categorized as being within the TSHR protein or the lipid region by calculating the circular variance (CV) of the entry and exit points of the protein since the CV was shown to be capable of determining whether a point is inside/outside/around the boundary of a set of points forming an irregular shape (20). The CV calculation used only the coordinates of the seven-helix bundle, projected onto the membrane plane (2D-CV).

Internal waters: The average number of waters inside the TMD were obtained by calculating the CV of each water of each frame saved in the trajectory w.r.t. the TMD and keeping the ones whose CV were above the threshold.

Measurement of cell volume changes using calcein fluorescence quenching: Water is transported within eukaryotic cells by passive diffusion and/or active transport when there is an osmotic change. This occurs via water channels known as aquaporins. The concept of cell volume changes due to water flux measured using calcein fluorescence is represented in Figure 1. The assay was performed using a rat thyrocyte line (FRTL5) and CHO cells overexpressing the human TSHR (21). Bovine TSH (Millipore Sigma, MA USA) which binds with high affinity to human and rat TSHR was used for activating the receptors. For the assay, 40,000 thyrocyte cells were seeded per well of clear bottom black 96 well plates and allowed to grow overnight in TSH-containing (6H) medium as described earlier. After attaining 80-90% confluency, the medium was

changed to TSH-free (5H) medium for 2 days to remove the effect of TSH. Prior to the assay the cells were first loaded with calcein AM at 5μM concentration in the presence of an inhibitor of anion transport (1mM probenecid) for 90 minutes at 37°C. Calcein, which is a non-fluorescent dye, becomes a fluorescent dye by cleavage due to intracellular esterases (44). The loaded cells are then washed twice with 37°C warm medium. To block both AQP1 and AQP4, the cells were further incubated for 30 minutes at 37°C with medium containing AQP1 inhibitor (TC- Tocris Cat # 5412) at 8μM and/or AQP4 inhibitor (TGN020 - Tocris Cat # 5425) at 3μM. After decanting the medium from the aquaporin blocked cells, the wells were then loaded with 50ul of medium containing either TSH, stimulating TSH receptor antibodies (MS1 at 10μg/ml and M22 at 1μg/ml) or TSHR small molecule agonists MS437/MS438 at 10μM in triplicates and incubated further for 20 minutes at 37°C. The plates were shifted immediately to a pre warmed microplate reader and the kinetic preset program started with an initial read of 5 sec followed by the injection of 50 μl of D-mannitol (400mM) resulting in a hyperosmotic extracellular milieu. An initial read at 5 sec for each well was followed by the 50μl injection of mannitol at a speed of 300μl/sec followed by a 37 sec continuous read of fluorescence for each well via bottom well optics. The average decrease or increase in fluorescence was calculated from measurements in triplicate wells for each treatment or no treatment using the excitation wavelength of 485 nm and emission wavelength of 525 nm. The data are presented as percentage change over control cells. Control percentage (100%) represented in the data refers to either a) maximum fluorescence of cells not subjected to hypertonic mannitol and not treated with aquaporin inhibitor(s) or b) maximum fluorescence of cells subjected to mannitol and in the presence of both aquaporin inhibitors depending on the experimental situation. The increase or decrease in the average fluorescence measured refers to equivalent changes in cell volume because calcein fluorescence decreases with aggregation of the

dye molecules and, in contrast. The fluorescence increases with dispersion of the molecules in this short time scale as illustrated in Figure 1 following their increased exposure to intracellular esterases.

Detection of aquaporins by PCR: FRTL5 cells grown in TSH-free 5H medium for 2 days were harvested and total RNA extracted using the RNA Easy kit (Qiagen cat # 74004). The RNA was further subject to column DNAase treatment to remove genomic DNA. 5µg of total RNA was converted to cDNA using the reverse transcriptase reaction using a SuperScript IV VILO cDNA kit (Thermo Fisher Inc). The cDNA was further diluted 1:3 and 2µl of diluted cDNA was then subjected into a PCR reaction using custom designed primer pairs for AQP1 and AQP4 (Supplementary Table S1 (22)). The PCR products were then run on 2% agarose gels for visualization of the amplified products. Primers for the cytoskeleton actin and beta- macroglobulin were used as controls.

Immunostaining for aquaporins 1 & 4: The presence of aquaporin protein expression was ascertained by immunostaining (22) using commercial polyclonal aquaporin antibodies for AQP1 using anti AQP1 (Proteintech Cat# 20333-1-AP, RRID:AB_10666159) and AQP4 using anti AQP4 (Proteintech Cat# 16473-1-AP, RRID:AB_2827426). Briefly, FRTL 5 cells grown on 8-well chamber slides with a density of 40,000 cells per well were washed twice with 1xPBS and fixed in 4% paraformaldehyde for 20 minutes at room temperature. The washed cells were then stained using a 1:200 dilution of the primary aquaporin antibody followed by 1hr incubation at room temperature. Bound primary antibody was detected using anti rabbit conjugate with Alexa 547 (1:500) (Jackson ImmunoResearch Labs Cat# 711-585-152, RRID:AB_2340621). The cells

were mounted using Vectashield containing Dapi for nuclear staining of cells. As controls we used FRTL5 cells stained with normal rabbit IgG followed by secondary antibody. Images of the cells were acquired using a Nikon Ti E wide field microscope using a 100x oil objective plan Apo with NA 1.45 and using Dapi and Texas red filters. Images were processed using the open-source Fuji Image J software. Minor adjustments were made on the images only for brightness and contrast.

Data analysis and statistical methods used: All experimental data were derived from 2-3 biological replicates all experiments. Were repeated 2-3 times. Statistical significance was calculated using the Student t test in Excel.

RESULTS

Identification of generic water sites associated with the TSHR TMD: Figure 2 (A-C) shows the TSHR-TMD models employed and illustrate three sets of generic water sites with occupancy greater than 30% corresponding to the three representative TMD structures in our earlier TRIO model (6). We found that the generic sites, when based on the third structure of the TRIO model (**Figure 2C**) (6), which represented more than half on the trajectory, formed a contiguous path between helices 6 and 7, reaching halfway from the intracellular side and an analogous shorter channel between helices 5 and 3 from the extracellular side. This suggested that waters could transit the membrane by passing through the interior of the TSHR protein as shown. Note, also, that the generic sites showed that there may be a path branching from the main path near the center of the bilayer, leading into the bilayer interior.

Simulation assesment of TSHR-TMD water transit: The appearance of the contiguous chain of water sites suggested we could track individual waters to detect their actual passage through the membrane. The result of tracking showed that during a 600 ns simulation there were 370 water transits observed (the number of waters in the system was 15,371) representing 2.4% of the waters in the system. However, only 188/370 (50.8%) of transits occurred through the receptor protein. Of the remaining transits, 87 occurred entirely through the DPPC bilayer and 95 occurred using a path that used the TSHR protein channel only for exit or entry. The average time required for the transit was extracted from the simulation history. It turned out to be 16.3 ns for the transit through the TSHR protein, 13.5 ns for the transit using partially the protein and lipid bilayer, and only 1.2 ns for the transit across the lipid bilayer. While the water channel transport time observed in the simulation via the TSHR protein was longer than via the lipid bilayer itself we found that significantly more waters traversed the bilayer via the TSHR than via the cell membrane. This is illustrated by straight lines connecting the entry and exit points as shown in **Figure 3**. Naturally, this does not imply that the path was a straight line, only to give a general sense of the distribution of the location and direction of transits. Transits that only partially use the TSHR appear to exit the protein into the membrane in the region where the generic water sites form a diverging path. The figure also shows that the transit lines involving the TSHR protein form two distinct bundles while the lines representing membrane bilayer transits are scattered and show significant lateral movements inside the bilayer. The lack of a contiguous water path in the first representative structure from our TRIO model (**Figure 2A**) is a reminder that the starting structure we actually used for the simulation is a homology model, based on proteins that may not always have a defined

path for the waters. The number of waters within the TMD of the different systems studied (**Table 1**) follows a similar pattern.

Specificity of transit modelling: The existence of a water channel raises the question whether that channel can also facilitate the transit of ions. To examine this question, the potassium and chloride ions in the neutral model water system were also tracked. However, no ion transits were observed at all. Tracking just the entries, we found that the ions did indeed enter the membrane but did not transit. **Table 2** shows the number of ions reaching different depths. It was clear that, unlike for water, the ion entries were significantly shallower within the TSHR protein than within the membrane bilayer. Potassium penetrated both the bilayer and the protein deeper than chloride and for entries into the protein potassium favored the extracellular side and chloride the intracellular side. Also, given that three potassium ions were seen within 4 angstrom of the bilayer center during the 600 ns molecular dynamic run it is was likely that longer simulations of microseconds in length may have seen actual transits of some potassium ions.

Simulation with the full length TSHR bound to TSH: Analysis of our simulations of the full-length TSHR model with and without the TSH, rather than just the TMD, showed that the inclusion of TSH resulted in an increase by a factor of ~2.2 in the number of water transits via the TMD **(Table 3).** Furthermore, constitutive transit through the lipid bilayer was nearly 10-fold lower than the via the TSHR protein itself **(Table 3)** suggesting active transport of water through the TSHR channel in the presence of TSH.

Aquaporin expression: In order to study actual TSHR water transport we used a well-established rat thyrocyte cell line (FRTL5). Since aquaporins are the major water transporters in all eukaryotic

cells, we first researched RNA seq data derived from the Human Protein Atlas (https://www.proteinatlas.org/) and Rat Genome Database (https:// rgd.mcw.edu/) to evaluate the expression of the different aquaporin's that are distributed in human and rat thyroid tissue. Analysis and representation of normalized transcripts per million (nTPM) levels from these datasets are shown in **Figure 4A** and suggested that aquaporin 1 (AQP1) and aquaporin 4 (AQP4) messages were the predominant isoforms expressed in both rat and human thyroid tissue. We then confirmed the expression of these two aquaporins in FRTL5 cells by qPCR and immunostaining of fixed cells **(Figure 4B upper).** Amplified PCR products of ~150 bases were observed using two different primer sets for each aquaporin and on immunostaining we identified both peripheral and cytoplasmic distribution of these aquaporin proteins **(Figure 4B lower**).

Aquaporin blockade: To establish if these aquaporin water transporters could be chemically inhibited we used a calcein fluorescence assay as detailed in Materials and Methods and as explained in **Figure 1**. We first observed a significant decrease in cell volume (~60%) as a result of the hypertonic change in the external milieu of the cells **(Figures 5A & 5B).** In contrast, in the presence of specific aquaporin inhibitors in concentrations greater than their IC_{50} and under the same hypertonic conditions there was no decrease in cell volume **(Figures 5A & 5B)** during the 37 sec measurement window. This occurred with blockade of either aquaporin suggesting that the inhibitors were not highly specific in the conditions used.

TSH effects on receptor water transport: We confirmed the influence of TSH on water flow by *in-vitro* analyses carried out on FRTL5 cells in the presence of combined AQP1 and AQP4 inhibitors. These data showed a clear TSH dose-response induced change in cell volume under

hypertonic conditions causing more than a 50% reduction in cell volumes **(Figure 6A)**. The specificity of this regulation by TSH was verified by blocking the binding of TSH to its receptor using human blocking antibody K1-70 (23) which restored some of the cell volume towards its initial state (**Figure 6B**). This action of TSH was also evaluated in a non-thyroid cell using heterologous CHO cells transfected with the human TSHR and control CHO cells lacking the receptor. CHO cells retained the same aquaporin effects and their chemical inhibition was observed as in thyrocytes **(Supplementary Figures S1A and S1B** (22)). In the presence of TSH an even more exaggerated effect than seen with FRTL5 cells was observed in this overexpressed model with up to 80% volume reduction illustrating TSHR specific water channels are likely to be effective conduits of water transit in all TSHR expressing cells.

TSHR antibodies and agonists also affect water transit: Since the TSH ligand binds to the ectodomain of TSHR and induced an alteration in water transport, we also tested if other modes of TSHR activation would have a similar effect. We examined two well-characterized stimulating monoclonal antibodies to the TSHR using the calcein assay. MS1, a in-house hamster TSHR stimulating monoclonal antibody (24) was tested at a dose of up to 10µg/ml and M22 (23) a human stimulating TSHR monoclonal antibody was tested at a dose up to 1µg/ml. The results indicated that both these antibodies, like TSH itself, were able to cause significant decreases in cell volume of FRTL5 cells **(Figure 6C).** Hence**,** perturbation of the receptor ectodomain resulted in water transit from the cells most likely by affecting the TSHR TMD. This conclusion was confirmed by direct stimulation of the TMD by using the TSHR small molecule agonists MS437 and MS438 which we had identified earlier (25). These allosteric activators also induced a significant decrease in cell volume in the calcein assay when tested at their maximum activation dose of 10µM **(Figure 6C).**

Therefore, changes in the transmembrane either by direct stimulation as seen by the allosteric activators or via the ectodomian due to TSH or stimulating TSHR antibodies resulted in changes in water transit via the receptor.

Receptor activation motifs on the TSHR water channel: To examine if water transit via the water channel could be affected by published TMD activation motifs we mapped the two most well defined activation motifs - the CMxP on TM6 and NLxxD motif on TM2 (26) using our TSHR TMD model from the molecular dynamic simulation **(Figure 7)**. Overlaying these motifs with the water transit path, we noted that the path of the water transit through the helices fell within these activation motifs that may indeed affect activation of the receptor.

DISCUSSION

The TSH receptor (TSHR), which is central to G protein signaling in thyrocytes, resides as an integral membrane protein in a hydrated lipid bilayer environment in the plasma membrane. Crystallographic structures of the TSHR, both active and inactive (7,27-29) forms including the recent full-length cryo-EM (30) structure, have expanded our understanding of how the TSH ligand and TSHR autoantibodies bind to the receptor. However, these studies have not addressed the behavior of water molecules associated with the receptor because of the static 3D images obtained in such studies. In our attempt to further understand the behavior of the TSHR in a lipid embedded and hydrated environment, we further analyzed the molecular dynamic (MD) simulation studies which resulted in our previously reported transmembrane domain (TMD) model named TRIO (31) and an improved version of our recently reported full length TSHR structure (32). Using our previous experience in modeling and the MD simulations of the TSHR-TMD, we

identified a network of putative transmembrane water channels within the TSHR protein. In this report, we have examined the role of the receptor associated water molecules in-silico as well as in-vitro to begin to understand their physiological relevance to the receptor protein.

On further analyzing our molecular dynamics simulation, we identified the potential trajectory of water molecules crossing a model of the TSHR embedded in a plasma membrane, which provided evidence that water molecules could indeed cross the membrane via these well-defined putative receptor channels in the TMD (**Figure 2**). These receptor water channels were confined mostly within H6 and H7 which are the sites of reported activation motifs among other GPCRs (26) including the TSHR (33). Furthermore, the transit lines constructed from the trajectories of water molecules in this model identified a bifurcated channel associated with the TSHR indicating the presence of both a complete channel through the receptor protein and a partial protein- membrane channel suggesting novel routes for these receptor waters.

The presence of receptor water networks is common in GPCRs (34,35) although they have not been characterized in the TSHR. It has been reported, however, that water molecules may form a network with receptor residues and hydrophobic amino acid side chains and may be intimately involved in activation of a receptor (35). To confirm the physiologic relevance of these receptor water channels in thyrocytes and possibly other extra thyroidal TSHRs, we used changes in cell volume as a measure of water transport using a calcein quenching fluorescence assay (36). Furthermore, we found that TSH and other TSHR agonists enhanced the water flow from thyrocytes.

We first examined water transit across the protein and lipid bilayer in our simulation. Transit of water through the lipid bilayer plasma membrane model was expected since it has been well shown that water passes through cell membranes by passive diffusion or facilitated diffusion

in live cells. The speed and, especially the quantity, of such membrane transits are known to be influenced by a variety of factors such as temperature, pH, fatty acid composition of the membrane, level of hydration, cholesterol in the membrane and including the osmotic pressures on each side of the membranea (37,38). To obtain an estimate of the speed of waters passing through the membrane in our simulation we first observed that there were about 600 waters in a single layer of the ~4 nm membrane. In the 600 ns simulation we observed that over 80 waters would cross the membrane, so it would take 600*(600/80)=4500 ns to move across all 600 waters, resulting in a speed of 4/4500 nm/ns, or about 10^{-4} nm/ns. We then found that this time spent by waters in membrane transit was an order of magnitude less than for transfers involving the TSHR protein. The difference in the frequency of transits via the protein and via the membrane reflects the high activation barrier that the membrane headgroups form. The difference in the transit times reflects the fact that the membrane interior is purely hydrophobic and thus creates a largely flat energy surface while the inside is at least partially polar and, as a result, it has several local minima that the water needs time to proceed through. Recent experiments mirror this result (39) where waters moved orders of magnitude faster through a hydrophobic channel lined with fluorine than through water transporting protein channels like aquaporin channels. It seems that the hydrophobic environment, by lacking the option to form hydrogen bonds with waters, is more ‘slippery’ than the interior of the protein. Nevertheless, it is not transit time alone that determines water flow but also the quantity of transits. While the transport time observed in the simulation via the TSHR protein was longer than via the membrane itself we found that significantly more waters traversed the bilayer via the TSHR protein than exclusively via the lipid bilayer (see Table 2). To understand the effects of ligand TSH on this water transit, we then examined 2000 ns long simulations of the full length TSHR (32), with and without TSH. We saw a significant increase over constitutive

water transport through the receptor, indicating that the capacity of the receptor channels to move water more than doubled with the binding of TSH in our simulation.

Using the calcein assay we were then able to confirm that such simulations reflected the physiological activity of TSH where we found large changes in cell volume under TSH stimulation of both thyroid cells as well as control non-thyroid cells expressing the TSHR. These in vitro studies in thyrocytes and heterologous cells were performed after chemical blockade of the two major aquaporins found in thyrocytes. Aquaporins are major water transporting proteins in all eukaryotic cells and distribution of these aquaporins isoforms is heterogeneous (40). This effect was not only mirrored when TSH or a stimulating TSHR antibody bound to the ectodomain of the full-length TSHR but was also seen upon binding of allosteric activators to the receptor TMD.

Water passes non-specifically and with ease in membrane models as well as in actual physiologic assessments (41). This suggests that passage of water molecules in any other way, such as via the TSHR protein, may have a physiological relevance. Since water paths appear to be possible through a variety of GPCRs (42) what advantage would this have? Since such receptors are thought to have evolved for G protein signaling, we can assume that water passage through the TSHR must have signaling significance and could maintain, enhance or inhibit such TSH signaling. In addition, receptor activation, which follows TSH or stimulating TSHR autoantibody binding to the large extracellular domain, likely leads to a rearrangement of the transmembrane helices and possibly an extension or alteration of the water network from the ligand-binding extracellular surface to the cytoplasmic surface (42). However, the model presented here of the TSHR is one of a constitutively active GPCR (43). In fact, the TSHR is never quiescent and it is known that this constitutive activity resides within the TMD and is thought to be kept in check by the ectodomain (44). The activation mechanism of the TSHR TMD has been

examined by comparative modelling of the TSHR model with active and inactive structures of three other GPCRs (33). The rearrangement of helices and distortion of the conserved motifs leading to activation of the TSHR is similar to other GPCRs but the role of water has not been evaluated before. Hydrophilic contacts in the TMD are complimented by conserved water molecules localized close to highly conserved residues and constitute a network of intramolecular and water-mediated interactions that could indeed be important for stabilizing the GPCR structure by linking the transmembrane helixes (34). Studies have shown that GPCRs have highly conserved motifs in their TMD and one such motif is the "ionic lock" (26). Additionally, the motif NLxxD in TM2 and CWxP in TM6 are important in maintaining the inactive state of some receptors (33) and any perturbation of these motifs by movement of water during activation could lead to changes in hydrogen bonding of the network and receptor activation or stabilization of the helixes (35). On mapping these well characterized activation motifs we found close proximity of these motifs with the TSHR water channel which suggested that they may play an active or surrogate role in TSHR signaling.

In conclusion, these observations evidence the integral role of water molecules in TSHR action and illustrate a new role for the TSH ligand itself. Although TSH action has been extensively characterized both by its interaction with the TSHR and its use of multiple G protein signaling molecules and pathways (45,46) its importance in fluid regulation has not been well described. Although one major characteristic of high TSH levels in hypothyroidism is one of fluid retention and effusion formation, especially pleural and pericardial effusions, these disease consequences have characteristically been blamed on lack of thyroid hormone (47). Yet there is a dearth of evidence exploring fluid transfer under different levels of TSH in the setting of widespread expression of the TSHR. Our description of TSHR water channels opens an entirely new way of

looking at fluid balance in hypothyroidism. This offers a new paradigm for TSH action as supported by the evidence that TSH can influence waters crossing into and out of the many cells expressing the receptor which would also include fibroblasts, osteoblasts and specialized brain cells such as tanycytes which express significant numbers of TSHR (48) and have a major contribution in hypothalamic hormone regulation (49).

Acknowledgments:

We thank Dr. Roman Osman for pointing out experimental information and for helpful discussions. This work was also supported in part through the computational resources and staff expertise provided by the Department of Scientific Computing at the Icahn School of Medicine at Mount Sinai.

Author contributions:

MM conceived the work, interpreted the simulation data and wrote the first draft of the manuscript. RL designed and executed the in vitro experiments and helped interpret the data, write and edit the figures and manuscript. TFD provided experimental planning, data interpretation and focus, helped prepare the figures and helped write the manuscript.

Data and materials availability: Initial structure coordinates and simulation trajectory are available from the authors upon e-mailed request. The programs MMC and Simulaid are available at the URL https://mezeim01.dmz.hpc.mssm.edu/software.html

References and Notes:

1. Worth CL, Kleinau G, Krause G. Comparative sequence and structural analyses of G-protein-coupled receptor crystal structures and implications for molecular models. *PLoS One*. 2009;4:e7011.
2. Rasmussen SG, DeVree BT, Zou Y, Kruse AC, Chung KY, Kobilka TS, Thian FS, Chae PS, Pardon E, Calinski D, Mathiesen JM, Shah ST, Lyons JA, Caffrey M, Gellman SH, Steyaert J, Skiniotis G, Weis WI, Sunahara RK, Kobilka BK. Crystal structure of the β2 adrenergic receptor-Gs protein complex. *Nature*. 2011;477:549-555.
3. T.E. Angel SG, B. Jastrzebskaa, K. Palczewski, and M.R. Chance. Structural waters define a functional channel mediating activation of the GPCR, rhodopsin. *PNAS*. 2009;106:14367–14372.
4. S. Yuan SF, K. Palczewski, and H. Vogel. Activation of G-protein-coupled receptors correlates with the formation of a continuous internal water pathway. *Nature Communications*. 2014;5.
5. A. J. Venkatakrishnan, Anthony K. Ma, Rasmus Fonseca, Dror RO. Diverse GPCRs exhibit conserved water networks for stabilization and activation. *Proc Natl Acad Sci U S A*. 2019;116(8):3288-3293.
6. Mezei M, Latif R, Das B, Davies TF. Implications of an improved model of the TSH receptor transmembrane domain (TSHR-TMD -TRIO). *Endocrinology*. 2021;162:bqab051
7. Faust B, Billesbølle CB, Suomivuori C-M, Singh I, Zhang K, Hoppe N, Pinto AFM, Diedrich JK, Muftuoglu Y, Szkudlinski MW, Saghatelian A, Dror RO, Cheng Y, Manglik A. Autoantibody mimicry of hormone action at the thyrotropin receptor. *Nature*. 2022;609:846-860.

8. Mezei M, Beveridge DL. Generic solvation sites in a crystal. *J Comp Chem*. 1984;6:523-527.

9. Ali MR, Latif R, Davies TF, Mezei M. Monte Carlo loop refinement and virtual screening of the thyroid-stimulating hormone receptor transmembrane domain. *Journal of Biomolecular Structure and Dynamics*. 2014:1-13.

10. Consortium TU. Reorganizing the protein space at the universal protein resource (UniProt). *Nucleic Acids Research*. 2012;50:D71-D75.

11. Cui M, Mezei M, Osman R. Prediction of protein loop structures using a local move Monte Carlo approach and a grid-based force field. *Protein Eng Des Sel*. 2008;21:729-735.

12. Mezei M. Grand-Canonical Ensemble Monte Carlo Simulation of Dense Fluids: Lennard-Jones, Soft Spheres and Water. *Mol Phys*. 1987;61:565-582.

13. Speidel JA, Banfelder JR, Mezei M. Automatic Control of Solvent Density in Grand Canonical Ensemble Monte Carlo Simulations. *J Chem Theory and Comp*. 2006;2:1429-1434.

14. Mezei M. Simulaid: a simulation facilitator and analysis program. *J Comput Chem*. 2010;31(14):2658-2668.

15. Jo S, Kim T, Iyer VG, Im W. CHARMM-GUI: a web-based graphical user interface for CHARMM. *J Comput Chem*. 2008;29(11):1859-1865.

16. Jing Huang, Jr ADM. CHARMM36 all-atom additive protein force field: validation based on comparison to NMR data *J Comput Chem*. 2013;34:2135-2145.

17. Wu EL, Cheng X, Jo S, Rui H, Song KC, Dávila-Contreras EM, Qi Y, Lee J, Monje-Galvan V, Venable RM, Klauda JB, Im W. CHARMM-GUI Membrane Builder Toward Realistic Biological Membrane Simulations. *J Comput Chem*. 2014;35:1997–2004.

18. Phillips JC, Braun R, Wang W, Gumbart J, Tajkhorshid E, Villa E, Chipot C, Skeel RD, Kale L, Schulten K. Scalable molecular dynamics with NAMD. *J Comput Chem*. 2005;26(16):1781-1802.

19. Mezei M. MMC: Monte Carlo program for molecular assemblies. URL: https://mezeim01.u.hpc.mssm.edu/mmc.

20. Mezei M. A new method for mapping macromolecular topography. *J Mol Graph Model*. 2003;21(5):463-472.

21. Solenov E, Watanabe H, Manley GT, Verkman AS. Sevenfold-reduced osmotic water permeability in primary astrocyte cultures from AQP-4-deficient mice, measured by a fluorescence quenching method. *Am J Physiol Cell Physiol*. 2004;286(2):C426-432.

22. Latif R. Supplementary Material. 2023.

23. Evans M, Sanders J, Tagami T, Sanders P, Young S, Roberts E, Wilmot J, Hu X, Kabelis K, Clark J, Holl S, Richards T, Collyer A, Furmaniak J, Smith BR. Monoclonal autoantibodies to the TSH receptor, one with stimulating activity and one with blocking activity, obtained from the same blood sample. *Clin Endocrinol (Oxf)*. 2010;73(3):404-412.

24. Ando T, Latif R, Pritsker A, Moran T, Nagayama Y, Davies TF. A monoclonal thyroid-stimulating antibody. *J Clin Invest*. 2002;110(11):1667-1674.

25. Latif R, Ali MR, Ma R, David M, Morshed SA, Ohlmeyer M, Felsenfeld DP, Lau Z, Mezei M, Davies TF. New small molecule agonists to the thyrotropin receptor. *Thyroid*. 2015;25(1):51-62.

26. Fritze O, Filipek S, Kuksa V, Palczewski K, Hofmann KP, Ernst OP. Role of the conserved NPxxY(x)5,6F motif in the rhodopsin ground state and during activation. *Proc Natl Acad Sci U S A*. 2003;100(5):2290-2295.

27. J. Miller-Gallacher PS, S. Young, A. Sullivan, S. Baker, S.C Reddington, M. Clue, K. Kabelis, J. Clark, J. Wilmot, D. Thomas, M. Chlebowska, F. Cole, E. Pearson, E. Roberts, M. Holly, M. Evans, R. Núñez Miguel, M. Powell, J. Sanders, J. Furmaniak, B. Rees Smith. Crystal structure of a ligand-free stable TSH receptor leucine-rich repeat domain. *Journal of Molecular Endocrinology* 2019;62:117–128

28. Sanders P, Young S, Sanders J, Kabelis K, Baker S, Sullivan A, Evans M, Clark J, Wilmot J, Hu X, Roberts E, Powell M, Nunez Miguel R, Furmaniak J, Rees Smith B. Crystal structure of the TSH receptor (TSHR) bound to a blocking-type TSHR autoantibody. *J Mol Endocrinol*. 2011;46(2):81-99.

29. J.Sanders, Chirgadze DY, Sanders P, Baker S, Sullivan A, Bhardwaja A, Bolton J, Reeve M, Nakatake N, Evans M, Richards T, Powell M, Miguel RN, Blundell TL, Furmaniak J, Smith BR. Crystal structure of the TSH receptor in complex with a thyroid-stimulating autoantibody. *Thyroid*. 2007;15(5):395-410.

30. Nunez Miguel R, Sanders P, Allen L, Evans M, Holly M, Johnson W, Sullivan A, Sanders J, Furmaniak J, Rees Smith B. Structure of full-length TSH receptor in complex with antibody K1-70. *J Mol Endocrinol*. 2023;70(1).

31. M. Mezei RL, B. Das, T.F. Davies. Implications of an improved model of the TSH receptor transmembrane domain (TSHR-TMD -TRIO). *Endocrinology*. 2021;162:bqab051

32. Mezei M, Latif R, Davies TF. Computational model of the full-length TSH receptor. *Elife*. 2022;11.

33. Nunez Miguel R, Sanders J, Furmaniak J, Smith BR. Structure and activation of the TSH receptor transmembrane domain. *Auto Immun Highlights*. 2017;8(1):2.

34. Louet M, Casiraghi M, Damian M, Costa MG, Renault P, Gomes AA, Batista PR, M'Kadmi C, Mary S, Cantel S, Denoyelle S, Ben Haj Salah K, Perahia D, Bisch PM, Fehrentz JA, Catoire LJ, Floquet N, Baneres JL. Concerted conformational dynamics and water movements in the ghrelin G protein-coupled receptor. *Elife*. 2021;10.

35. Tomobe K, Yamamoto E, Kholmurodov K, Yasuoka K. Water permeation through the internal water pathway in activated GPCR rhodopsin. *PLoS One*. 2017;12(5):e0176876.

36. Kitchen P, Salman MM, Abir-Awan M, Al-Jubair T, Tornroth-Horsefield S, Conner AC, Bill RM. Calcein Fluorescence Quenching to Measure Plasma Membrane Water Flux in Live Mammalian Cells. *STAR Protoc*. 2020;1(3):100157.

37. Haines TH. Water transport across biological membranes. *FEBS Letters*. 1994;346:115-122.

38. Verkman AS, van Hoek AN, Ma T, Frigeri A, Skach WR, Mitra A, Tamarappoo BK, Farinas J. Water transport across mammalian cell membranes. *Am J Physiol*. 1996;270(1 Pt 1):C12-30.

39. Itoh Y, Chen S, Ryota H, Konda T, Aoki T, Ueda T, Shimada I, Cannon JJ, Shao C, Shiomi J, Tabata KV, Noji H, Sato K, Aida T. Ultrafast water permeation through nanochannels with a densely fluorous interior surface. 2022.

40. Azad AK, Raihan T, Ahmed J, Hakim A, Emon TH, Chowdhury PA. Human Aquaporins: Functional Diversity and Potential Roles in Infectious and Non-infectious Diseases. *Front Genet*. 2021;12:654865.

41. Blankenship E, Lodowski AV-FDT. The high-resolution structure of activated opsin reveals a conserved solvent network in the transmembrane region essential for activation. *Struvture*. 2015;23:2358-2364.

42. Angel TE, Chance MR, Palczewski K. Conserved waters mediate structural and functional activation of family A (rhodopsin-like) G protein-coupled receptors. *Proc Natl Acad Sci U S A*. 2009;106:8555–8560.

43. Katritch V, Fenalti G, Abola EE, Roth BL, Cherezov V, Stevens RC. Allosteric sodium in class A GPCR signaling. *Trends Biochem Sci*. 2014;39:233–244.

44. Neumann S, Claus M, Paschke R. Interactions between the extracellular domain and the extracellular loops as well as the 6th transmembrane domain are necessary for TSH receptor activation. *Eur J Endocrinol*. 2005;152(4):625-634.

45. Laugwitz KL, Allgeier A, Offermanns S, Spicher K, Van Sande J, Dumont JE, Schultz G. The human thyrotropin receptor: a heptahelical receptor capable of stimulating members of all four G protein families. *Proc Natl Acad Sci U S A*. 1996;93(1):116-120.

46. Morshed SA, Latif R, Davies TF. Characterization of thyrotropin receptor antibody-induced signaling cascades. *Endocrinology*. 2009;150(1):519-529.

47. Kinoshita H, Ishii A, Hayakawa A, Yasuda M, Inoshita S, Yakushiji F. Severe hypothyroidism associated with the degree of edema in a patient with nephrosis. *Clin Pract*. 2011;1(3):e78.

48. Kannangara H, Cullen L, Miyashita S, Korkmaz F, Macdonald A, Gumerova A, Witztum R, Moldavski O, Sims S, Burgess J, Frolinger T, Latif R, Ginzburg Y, Lizneva D, Goosens K, Davies TF, Yuen T, Zaidi M, Ryu V. Emerging roles of brain tanycytes in regulating blood-hypothalamus barrier plasticity and energy homeostasis. *Ann N Y Acad Sci*. 2023.

49. Langlet F. Tanycytes: a gateway to the metabolic hypothalamus. *J Neuroendocrinol*. 2014;26(11):753-760.

.

Figures and Legends

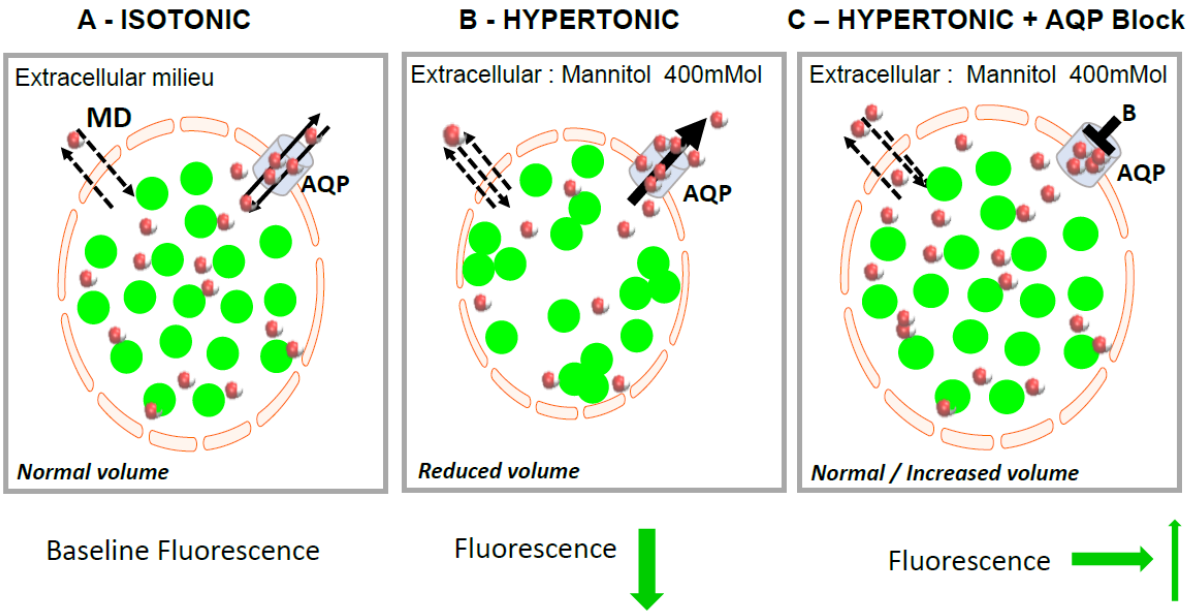

Figure 1: Measuring Cell Volume Changes Using the Calcein Quenching Assay

Calcein becomes a fluorescent molecule within cells and its fluorescence is reduced as the calcein molecules aggregate together. In a short time scale, the concentration - dependent fluorescence of calcein can be used as a probe for studying cell volume changes. (A) Under isotonic conditions the cell maintains a normal volume and a basal calcein fluorescence. (B) Under induced hypertonic conditions caused by the addition of 400mM of D -mannitol to the extracellular milieu, water molecules transit out of the cell very actively via aquaporin channels (AQPs) and more slowly through cell membrane diffusion (MD) leading to a decrease in cell volume reflected by a decrease in calcein fluorescence as a result of increased aggregation of calcein molecules. (C) In the presence of chemical blockers of the AQPs, this water transit is stopped, and cells lose much less water molecules only by diffusing through the plasma membrane and this prevents a major decrease in volume and little change in fluorescence. MD = membrane diffusion, AQP = Aquaporins and B = Blocker

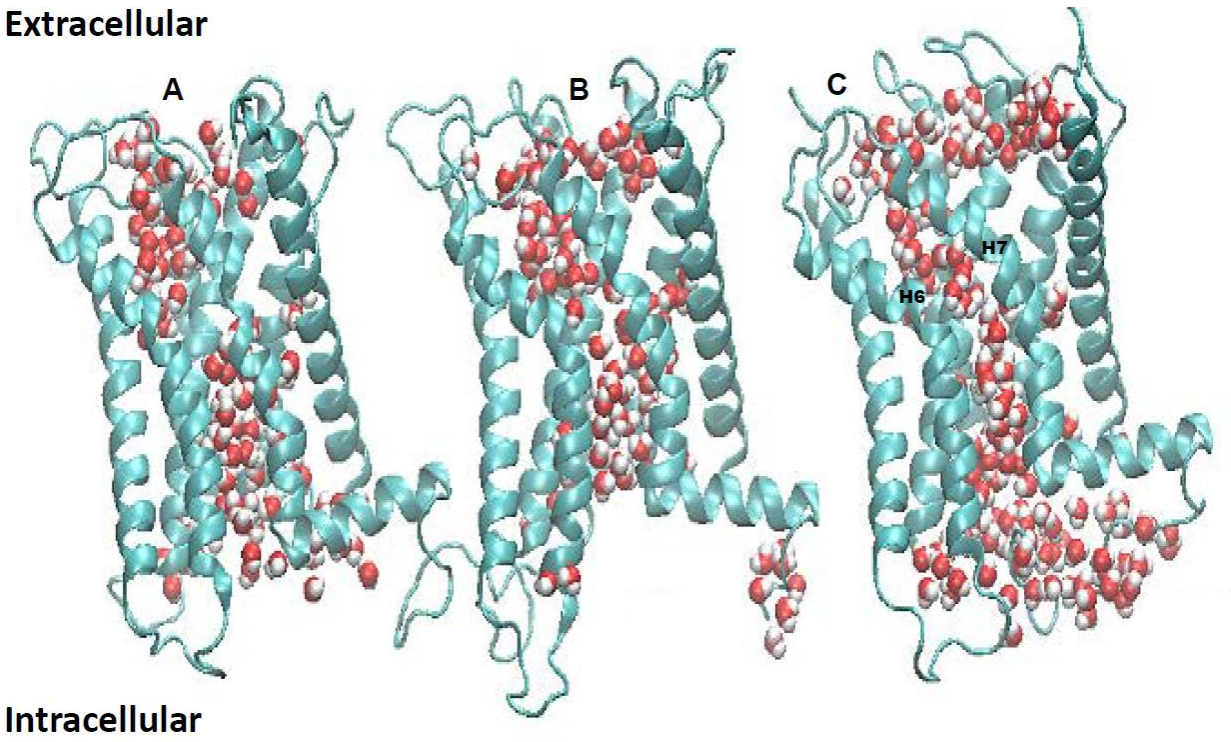

Figure 2: Representation of Water Transit through the TSHR TMD

Shown are representative structures of the three clusters of the simulated trajectory in the TRIO models (A, B and C) with the site waters shown in red. The waters represent generic sites with occupancy > 0.3 for the three TRIO structures from the 600 ns MD simulation. The helices of the TMD are shown in blue with water molecules represented by red oxygen and white hydrogen atoms which trace a channel through the TSHR-TMD.

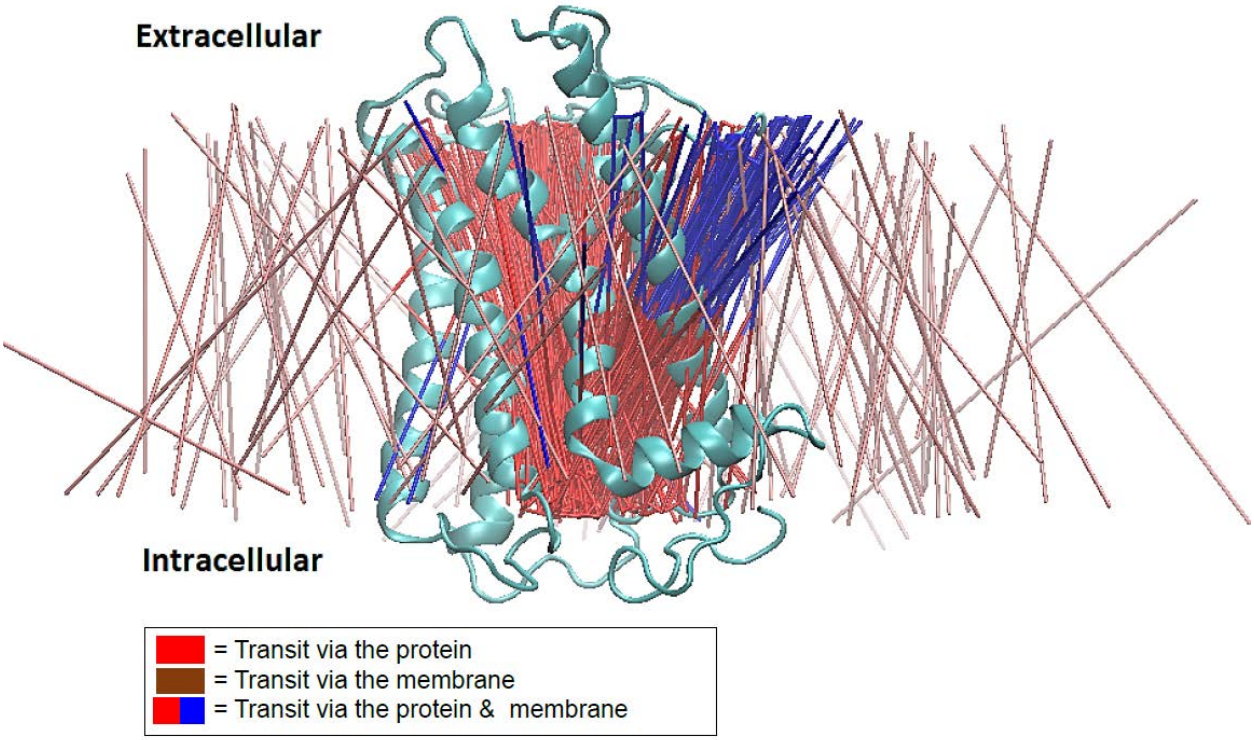

Figure 3: **Transit Lines of Water Movement in the Membrane- Embedded TMD**

This diagram shows the lateral view of the transit lines extracted from the MD simulation data representing 370 transits observed. The brown lines represent transit (diffusion) via the membrane, the red lines represent transit via the TSHR protein only and the blue lines represent the path branching from the TSHR-TMD protein into the membrane suggesting a bifurcated transit of the waters.

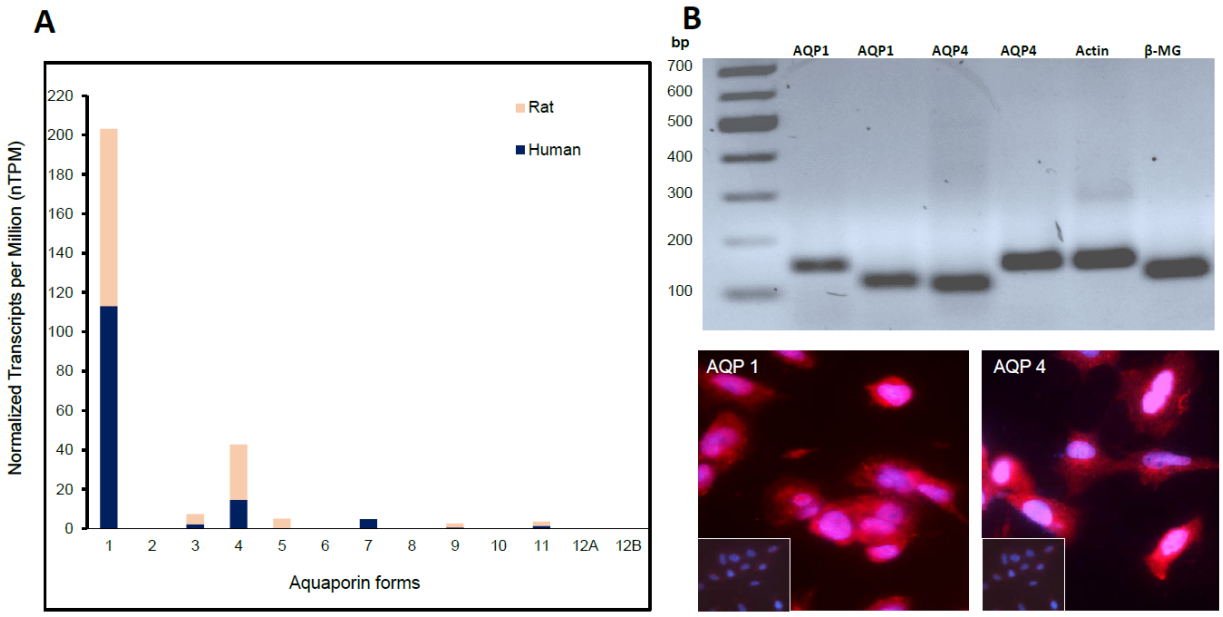

Figure 4: **Aquaporins Expressed in Thyrocytes**

Aquaporins represent the classical water transporting units found in most cells and which are found in different isoforms. We identified and confirmed the major isoforms that are present in thyrocytes**. (A)** The stack bars (black) are data extracted from the Human Protein Atlas (https://www.proteinatlas.org/) for different aquaporin mRNAs present in thyroid tissue. The beige colored bars represent similar data derived for rat thyroid tissue from the Rat Genome database (https://rgd.mcw.edu/) These data demonstrated that AQP 1 and 4 are the major forms to be found in thyroid cells. (B) Confirmation of the expression of AQP1 and AQP 4 was obtained by PCR using two sets of primers for each aquaporin with actin and β microglibulin as positive controls as shown the gel image. A 100base pair ladder is shown on the left. The lower images are of FRTL5 cells grown on glass chamber slides and fixed in paraformaldehyde and then stained with AQP1 and AQP4 rabbit polyclonal antibodies. The primary antibody was detected using anti rabbit IgG conjugated

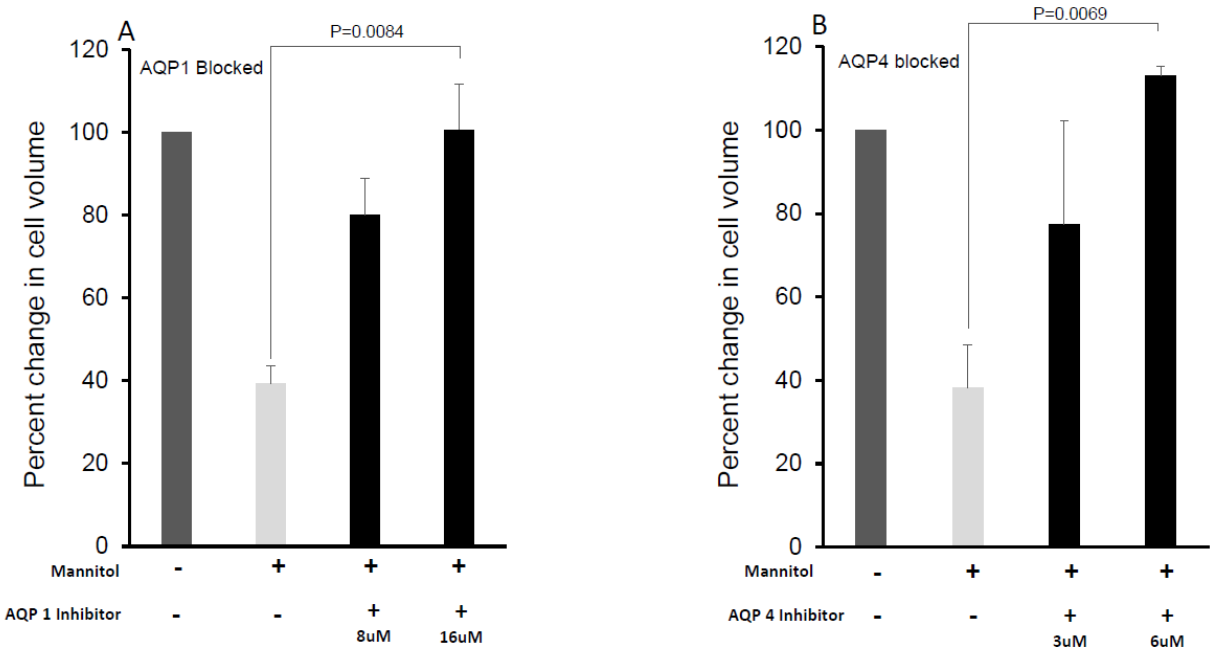

Figure 5: Assessment Of Aquaporin Blockade In FRTL5 Cells

In order to specifically examine TSHR water channel effects in vitro using the calcein assay we had to first assess the chemical blockade of aquaporin using inhibitor molecules. FRTL5 cells grown on clear bottom black 96 well plates were subjected to the calcein assay in the absence and presence of AQP1 and AQP 4 inhibitors. The data shown are the average of two experiments (n=2) and are shown as the percentage change in cell volume compared to the baseline control cells (100%) = No mannitol +No AQP Inhibitors. (**A & B)** Cells in the presence of mannitol and no inhibitor showed a 60% decrease in cell volume which was restored to normal levels with concentrations of >IC_{50} of either AQP inhibitors showing good blockade of the primary aquaporins in these rat thyrocytes.

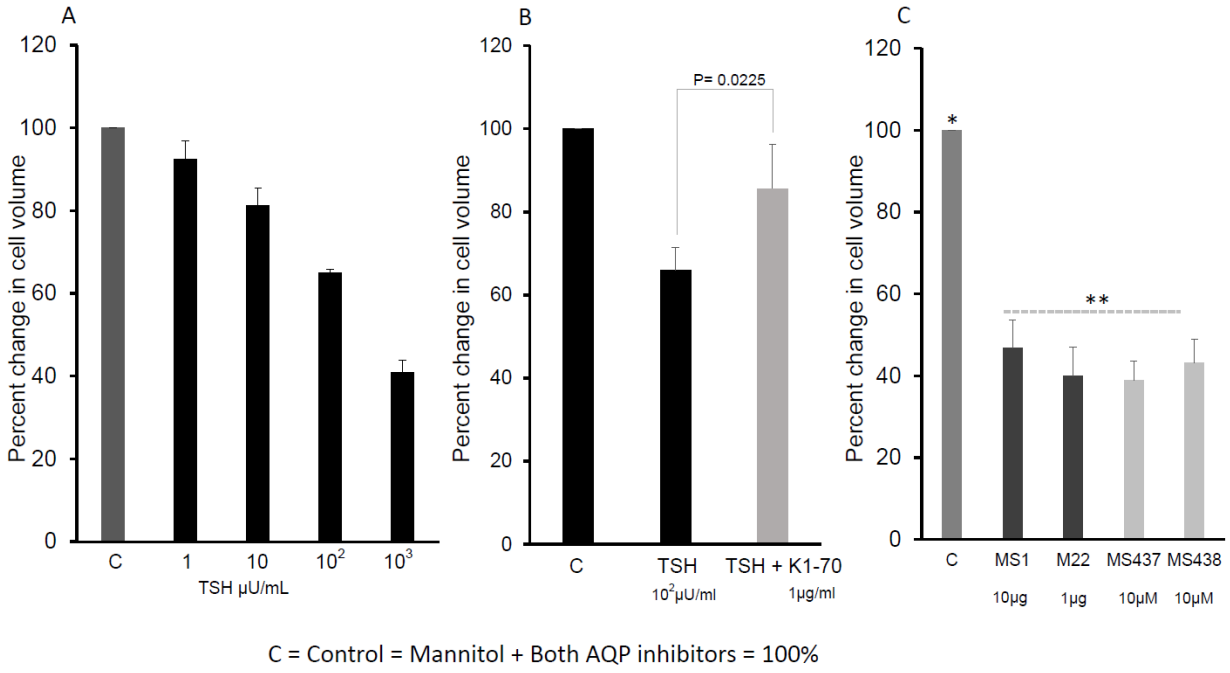

Figure 6: Effect Of Ectodomain and Transmembrane Activation On Water Transport

The TSHR can be activated by TSH or stimulating TSHR autoantibodies that bind to its large extracellular domain (ECD) and also by allosteric small molecule that bind to sites within the "binding pocket" of the TMD. Using the calcein fluorescence assay after blockade of AQPs 1 & 4, we tested the effect of increasing concentrations of TSH on water transit in FRTL5 cells deprived of TSH at different doses (**A**). This effect of TSH could be neutralized by adding a blocking antibody **(B)**. Furthermore, we also tested stimulating monoclonal antibodies at their maximum effective dose and our previously described novel small molecule agonists (**C**)(25). A dose-response with TSH on cell volume changes was observed with 10^2 and 10^3 µU/mL of TSH with significant reductions in cell size of 40-60%. Similar changes were seen with two stimulating TSHR monoclonal antibodies and with our TSHR agonist molecules MS437 and MS 438.

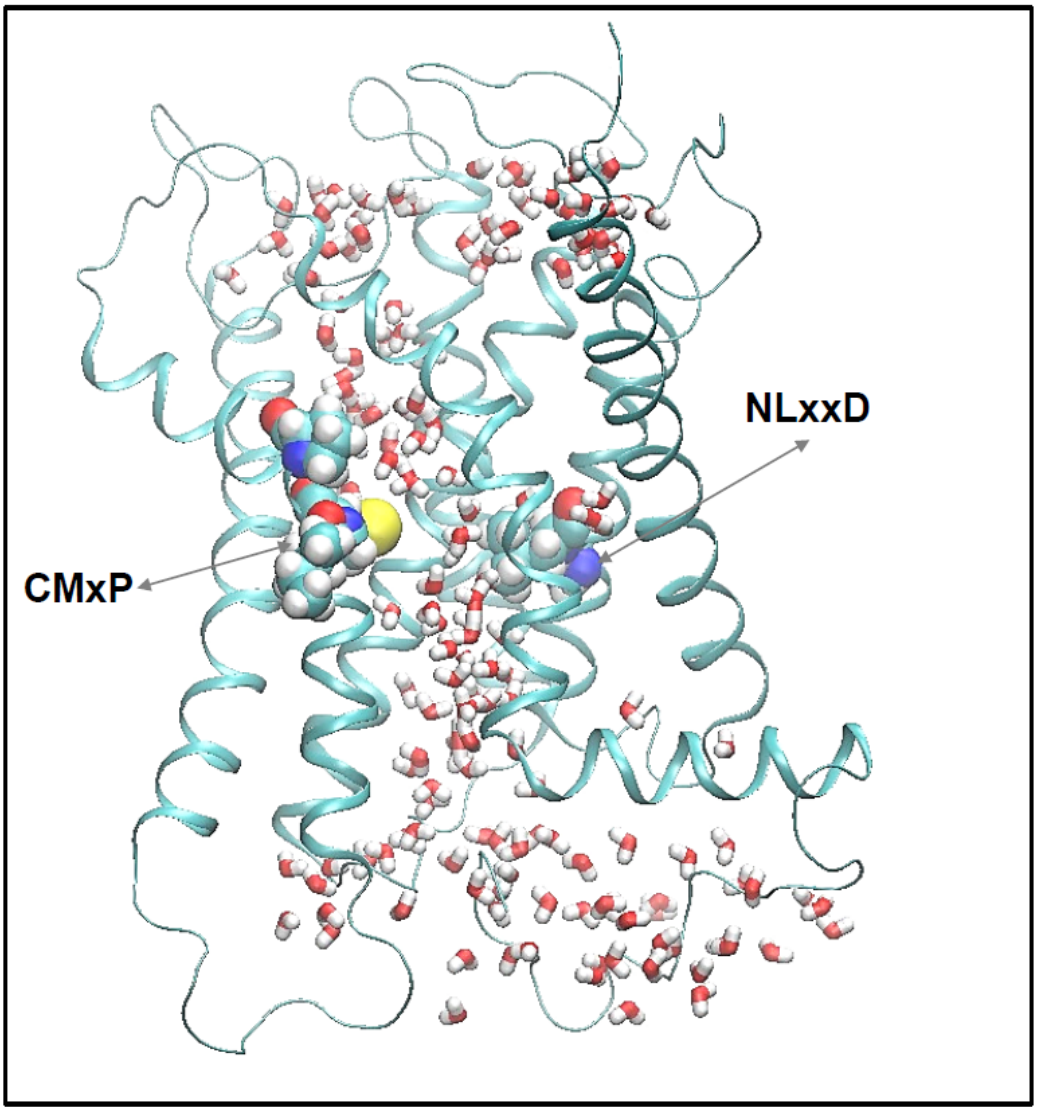

Figure 7: TSHR Activation Motif within Water Channel

The amino acid sequences of GPCRs are known to show some highly conserved motifs which are involved in receptor activation via the TMD. The NLxxxD motif in TM2 and the CWxP motif in TM6 are such motifs present in the TSHR-TMD structure. On mapping the water channel to these motifs we observed that the route of water transit is in close proximity to both of these motifs as shown in these lateral images of the TSHR TMD with helices in blue and motif residues represented by the enlarged residues in yellow, red and blue.

Table 1: Depth of ion entries into the TSHR-TMD and lipid bilayer

Depth / Å	TSHR-TMD, intra-cellular entry		TSHR-TMD, extra-cellular entry		Lipid bilayer	
	K^+	Cl^-	K^+	Cl^-	K^+	Cl^-
> 0	122	14	265	629	5853	1027
> 2	50	4	74	159	4150	283
> 4	24	0	17	5	2540	72
> 6	8	0	0	0	1342	15
> 8	1	0	0	0	547	4
> 10	0	0	0	0	150	0
> 12	0	0	0	0	26	0
> 14	0	0	0	0	5	0
> 16	0	0	0	0	3	0
> 18	0	0	0	0	0	0

Table 2: Number of membrane transits of different types

TRANSIT TYPE	FL TSHR (-TSH)	FL TSHR (+TSH)	TMD	TMD (scaled)
	2000 ns	2000 ns	600 ns	2000 ns
TSHR Protein	4,948±415	11,411±1162*	202±31	673
Lipid bilayer	293±31	632±28	88±15	293
Memb:TSHR	220±40	380±77	41±17	136
TSHR:Memb	205±194	414±68	39±11	129

FL = Full length, TMD= transmembrane domain, * ±TSH – $p < 0.0001$

Table 3: Average number of waters actually inside the TMD enhanced by TSH

	TSHR (2000 ns)		TSHR-TSH (2000 ns)		TMD (300 ns)	
CV_{min}	$<N_w>$	Range	$<N_w>$	Range	$<N_w>$	Range
0.85	55.4±12.6	[20,97]	107.1±13.1	[75,158]	55.7±11.7	[15,85]
0.87	43.5±11.9	[16,85]	78.1±18.7	[34,146]	49.4±11.0	[12,75]

CV_{min} = the circular variance threshold used to filter the waters

N_w = Number of waters

List of Supplementary Materials

Supplementary Figure S1: Cell shrinkage induced by TSH in CHO:TSHR cells

Supplementary Table S1: Premade primer pairs employed